Effects of anisotropy and Coulomb interactions on quantum transport in a quadruple quantum-dot structure

M. Yu. Kagan,[1,2,*] V. V. Val'kov,[3,†] and S. V. Aksenov[3,‡]

[1]*P. L. Kapitza Institute for Physical Problems RAS, 119334 Moscow, Russia*

[2]*National Research University Higher School of Economics, 101000 Moscow, Russia*

[3]*Kirensky Institute of Physics, Federal Research Center KSC SB RAS, 660036 Krasnoyarsk, Russia*

(Received 4 October 2016; revised manuscript received 24 November 2016; published 11 January 2017)

We present an analytical and numerical investigation of the spectral and transport properties of a quadruple quantum-dot (QQD) structure which is one of the popular low-dimensional systems in the context of fundamental quantum physics study, future electronic applications, and quantum calculations. The density of states, occupation numbers, and conductance of the structure were analyzed using the nonequilibrium Green's functions in the tight-binding approach and the equation-of-motion method. In particular the anisotropy of hopping integrals and on-site electron energies as well as the effects of the finite intra- and interdot Coulomb interactions were investigated. It was found out that the anisotropy of the kinetic processes in the system leads to the Fano-Feshbach asymmetrical peak. We demonstrated that the conductance of the QQD device has a wide insulating band with steep edges separating triple-peak structures if the intradot Coulomb interactions are taken into account. The interdot Coulomb correlations between the central QDs result in the broadening of this band and the occurrence of an additional band with low conductance due to the Fano antiresonances. It was shown that in this case the conductance of the anisotropic QQD device can be dramatically changed by tuning the anisotropy of on-site electron energies.

DOI: 10.1103/PhysRevB.95.035411

I. INTRODUCTION

Low-dimensional systems attract significant attention from researchers with both the possibility to study fundamental quantum physics and potential applications in nanoelectronics. One of the basic objects there are quantum dots (QDs). Different, often coexisting processes such as the Kondo, Fano, and Aharonov-Bohm effects as well as the Hubbard model physics are probed in the systems of QDs [1–3]. In the single-electron regime these structures are proposed to be utilized as spin qubits [4,5]. In addition, it was shown that they can act as rectifiers, spin filters, and valves [6].

Among QD-based structures, the arrays containing three and more QDs have been actively studied only recently due to more difficult experimental realization [7,8]. The structures consisting of four QDs, quadruple quantum-dot (QQD) structures, were explored in different geometries. A nanosecond-time-scale spin transfer of individual electrons across the serially connected QQD device was reported in [9]. In a squarelike configuration such an operation was demonstrated on a closed path inside the QQD system [10]. In the same system with three electrons Nagaoka's ferromagnetism was observed [11,12], the features of the spin exchange of four electrons were studied [13,14], and a self-contained quantum refrigerator was investigated [15]. It is important to emphasize that for all geometries the intra- and interdot Coulomb repulsion is a key factor influencing the spectrum and transport properties [16,17].

The most common situation for quantum transport measurements of the QQD structure is when left and right metal contacts are coupled with two QDs so that the other two QDs are situated in the central part (see Fig. 1). The investigation of the Fano, Aharonov-Bohm, and Aharonov-Casher interference effects in the Landauer formalism for this geometry earlier was restricted by the extreme cases of either strong Coulomb interaction (the Kondo regime) or the absence of it [18,19]. Meanwhile, it was shown in [19] that the QQD device subjected to the Rashba spin-orbit coupling acts as a spin filter. A similar behavior without the Rashba spin-orbit interaction and the Aharonov-Bohm effect was demonstrated for a multiple-QD network, the simplest case of which is the QQD [20]. In the last work the influence of the Coulomb interaction on the conductance was limited by the corresponding intradot term in the Hamiltonian. Thus the transport and spectral properties of the QQD structure in a more general regime when both the finite intra-, U, and interdot, V, Coulomb interactions and the anisotropy effects are taken into account have not been considered yet. The anisotropy implies the difference of the hopping integrals in the QQD or on-site carrier energies (due to, e.g., gate fields, V_{g1} and V_{g2}) which takes place in experiments.

Here it is important to note that the introduction of the anisotropy allows us to effectively consider the QQD structure as the two-band Hubbard system. Let us recall that usually the electron polaron effect (EPE) is present in multiband strongly correlated electron systems with substantially different electron bandwidths such as uranium-based heavy-fermion systems and other systems in mixed valence regimes [21–24] which can be described for example by the two-band Hubbard model with one narrow band (in the case of sufficiently strong interband Hubbard interaction V) [25,26] or the Anderson model (AM) [27] with one-particle hybridization (t_0 in our case) and two-particle Hubbard interaction between s-p electrons of the light band and (heavy) electrons of localized f-d levels. In the two-band Hubbard model EPE is usually

*kagan@kapitza.ras.ru

†vvv@iph.krasn.ru

‡asv86@iph.krasn.ru

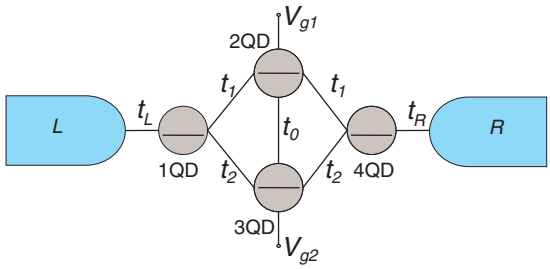

FIG. 1. The QQD structure between metallic leads.

connected with the additional polaronic narrowing of the heavy particles' bandwidth due to the dressing of the heavy particles in the virtual cloud of soft electron-hole pairs of the light particles. Similarly in the AM the EPE leads to the additional narrowing of the hybridization matrix element t_{12}. Note that in the QQD scheme (Fig. 1) t_{12} corresponds to the electron hopping t_2 from the 1QD to 3QD or correspondingly to the (reverse) hopping from the 3QD to the 4QD. Consequently in all our calculations we should effectively replace t_2 by $t_2' \ll t_2$ in the case of strong EPE produced by large values of V or t_0. Thus in numerical analysis we will suppose that the anisotropy is induced by both specific design of the structure and the above-mentioned many-body effects.

Note that the physics of EPE is closely connected with the well-known results of Kondo and Nozieres *et al.* on infrared divergences in the description of the Brownian motion of a heavy particle in a Fermi liquid of light particles [28,29] (see also the important results of Kagan and Prokof'ev [30,31]) as well as with the results on the infrared Mahan type [32] divergences for the problem of x-ray photoemission from the deep electron levels [33] and with the famous results of Anderson [34] on the orthogonality catastrophe for the 1D chain of N electrons in the presence of one impurity in the system.

In all the cases both in uranium-based heavy-fermion systems [25,26] and in other mixed valence systems such as manganite silicides, for example [35], EPE in the infinite geometry leads to anomalous resistivity characteristics in 3D and especially in 2D (layered) systems. Note that the manifestations of EPE are also very interesting in the restricted geometry of the tunnel junction (see the pioneering results of Matveev and Larkin [36]) when we consider a charge sector of intradot Coulomb correlations [37,38] and strong interdot Hubbard correlations between electrons in the central part (2- and 3QDs). As we will show in this case there should be additional Fano-Feshbach [39,40] resonances in the tunneling conductance and an effective one-particle density of states for the junction.

Here it is important to note an additional analogy between our system and the systems with impurities and defects. In real situations which are considered in the physics of electrical currents in dielectrics and semiconductors we are usually dealing with a small number of deep two-level traps surrounded by a large number of shallow traps with one level. In particular, a similar system, where deep two-level traps are randomly distributed between shallow one-level traps, is described in the well-known paper of Bishop's group [41] in connection with the physics of the radiation-induced conductivity (important for space applications) and more standard electron-phonon (or more exactly Holstein type configurational) polaron effects in molecularly doped polymers. In these terms our QQD structure can be treated as the simplest model with one central deep two-level trap (2- and 3QDs) in the surrounding of two shallow one-level traps (1- and 4QDs) in the restricted geometry of the junction, where, for the sake of simplicity, we neglect the peculiarities of the hopping conductivity on the Miller-Abrahams lattice.

In this article, on the basis of the nonequilibrium Green's function technique and the tight-binding approximation we studied spectral and transport characteristics of the QQD structure in which the intra- and interdot Coulomb correlations as well as the anisotropy effects take place. The interdot Coulomb interaction was considered between the QDs in the central part (see Fig. 1). In order to define the role of the Coulomb interactions in the formation of the transport properties beyond the mean-field approximation the decoupling scheme of You and Zheng [42,43] was adapted.

The paper has been organized into six sections. The model Hamiltonian is described in Sec. II. The nonequilibrium Green's function technique in the tight-binding approximation is presented in Sec. III. The analytical derivation of the retarded Green's functions of the QQD taking into account the Coulomb interactions is presented in Sec. IV. The results concerning the transport without the Coulomb interactions are presented in Sec. V. The influence of the Coulomb interactions is considered in Sec. VI. Conclusions are given in Sec. VII.

II. THE MODEL HAMILTONIAN

Let us consider electron quantum transport in the QQD structure depicted in Fig. 1. The system consists of three parts which are metallic leads and the structure between them. The Hamiltonian of the system is

$$\hat{H} = \hat{H}_L + \hat{H}_R + \hat{H}_D + \hat{H}_T. \tag{1}$$

The first two terms characterize the leads,

$$\hat{H}_{L(R)} = \sum_{k\sigma} \left(\xi_{k\sigma} \mp \frac{eV}{2} \right) c^+_{L(R)k\sigma} c_{L(R)k\sigma}, \tag{2}$$

where $c^+_{L(R)k\sigma}$ is the creation operator in the left (right) lead with quantum number k, spin σ, and spin-dependent energy $\xi_{k\sigma} = \epsilon_{k\sigma} - \mu$; μ is the chemical potential of the system. It is supposed that the voltage $\pm V/2$ is applied to the left (right) lead.

The third term describes the QQD structure,

$$\begin{aligned} \hat{H}_D = & \sum_{\sigma;j=1}^{4} \xi_{j\sigma} a^+_{j\sigma} a_{j\sigma} + U \sum_{j=1}^{4} n_{j\uparrow} n_{j\downarrow} \\ & + V \sum_{\sigma\sigma'} n_{2\sigma} n_{3\sigma'} + \sum_{\sigma} [t_1 (a^+_{1\sigma} + a^+_{4\sigma}) a_{2\sigma} \\ & + t_2 (a^+_{1\sigma} + a^+_{4\sigma}) a_{3\sigma} + t_0 a^+_{2\sigma} a_{3\sigma} + \text{H.c.}], \end{aligned} \tag{3}$$

where $a_{j\sigma}$ annihilates the electron with spin σ and energy $\xi_{j\sigma} = \epsilon_{j\sigma} - \mu$ on the jth QD; t_i, $i = 0,1,2$ is a hopping matrix element between the QDs; U is the intensity of the

intradot Coulomb interaction; V is the intensity of the interdot Coulomb interaction between the electrons in the central part (the 2nd and 3rd QDs). It is worth noting that such a specific type of the QQD structure with only one interdot Coulomb interaction can be experimentally received by using the conducting back gates near the peripheral QDs (1- and 4QDs) which would screen their charges [44].

The interaction between the leads and the QQD structure is determined by the last summand in (1),

$$\hat{H}_T = t_L \sum_{k\sigma} c^+_{Lk\sigma} a_{1\sigma} + t_R \sum_{k\sigma} c^+_{Rk\sigma} a_{4\sigma} + \text{H.c.}, \quad (4)$$

where $t_{L(R)}$ is a hopping matrix element between the left (right) lead and the 1st (4th) QD. Since the bias voltage is treated exactly it is convenient to perform a unitary transformation, $\hat{U} = \exp\{\frac{ieVt}{2} \sum_{k\sigma} (n_{Rk\sigma} - n_{Lk\sigma})\}$ [45], to insert it into the tunnel Hamiltonian,

$$\hat{H}_T = T_L(t) \sum_{k\sigma} c^+_{Lk\sigma} a_{1\sigma} + T_R(t) \sum_{k\sigma} c^+_{Rk\sigma} a_{4\sigma} + \text{H.c.}, \quad (5)$$

where $T_{L(R)}(t) = t_{L(R)} e^{\mp \frac{ieV}{2} t}$.

III. CURRENT AND NONEQUILIBRIUM GREEN'S FUNCTIONS IN THE TIGHT-BINDING APPROACH

To analyze transport properties of the system we utilize the nonequilibrium Green's function method in the tight-binding approximation [46–48]. Let us rewrite the Hamiltonian (1) in terms of the operators $\widehat{\psi}_{L(R)k}$ and $\widehat{\psi}_D$:

$$\widehat{\psi}_{L(R)k} = (c_{L(R)k\uparrow} c_{L(R)k\downarrow})^T, \widehat{\psi}_D = (a_{1\uparrow} a_{1\downarrow} \dots a_{4\uparrow} a_{4\downarrow})^T.$$

Then

$$\hat{H}_{L(R)} = \sum_k \widehat{\psi}^+_{L(R)k} \widehat{\xi}_k \widehat{\psi}_{L(R)k}, \hat{H}_D = \widehat{\psi}^+_D \widehat{h}_D \widehat{\psi}_D, \quad (6)$$

$$\hat{H}_T = T_L(t) \sum_k \widehat{\psi}^+_{Lk} \widehat{P}_1 \widehat{\psi}_D + T_R(t) \sum_k \widehat{\psi}^+_{Rk} \widehat{P}_4 \widehat{\psi}_D + \text{H.c.}, \quad (7)$$

where

$$\widehat{h}_D = \begin{pmatrix} \widehat{\xi}_1 & \widehat{t}_1 & \widehat{t}_2 & \widehat{0} \\ \widehat{t}_1 & \widehat{\xi}_2 & \widehat{t}_0 & \widehat{t}_1 \\ \widehat{t}_2 & \widehat{t}_0 & \widehat{\xi}_3 & \widehat{t}_2 \\ \widehat{0} & \widehat{t}_1 & \widehat{t}_2 & \widehat{\xi}_4 \end{pmatrix}, \quad (8)$$

$$\widehat{t}_i = \text{diag}(t_i), \widehat{\xi}_l = \text{diag}(\xi_{l\uparrow}, \xi_{l\downarrow}), l = k, 1, \dots, 4. \quad (9)$$

The operators $\widehat{P}_1 = (\widehat{I}\widehat{0})$ and $\widehat{P}_4 = (\widehat{0}\widehat{I})$ project matrices on the subspace related to the 1st and 4th QD, respectively. They consist of the 2×2 unitary matrix, $\widehat{I}$, and the zero block, $\widehat{0}$.

An electrical current operator in the left lead is determined by the corresponding charge change per time unit, $\widehat{I}_L = e\dot{N}_L$, where $N_L = \sum_{k\sigma} c^+_{Lk\sigma} c_{Lk\sigma}$ is the carrier number operator in the left lead. Using the equation of motion for Heisenberg operators $\langle \widehat{I}_L \rangle$ becomes

$$\langle \widehat{I}_L \rangle \equiv I_L = ie \sum_k \langle T^+_L \widehat{\psi}^+_D \widehat{P}^+_1 \widehat{\psi}_{Lk} - T_L \widehat{\psi}^+_{Lk} \widehat{P}_1 \widehat{\psi}_D \rangle. \quad (10)$$

Let us introduce the nonequilibrium matrix Green's functions as

$$\widehat{G}^{ab}_{nm}(\tau, \tau') = -i \langle \hat{T}_C \widehat{\psi}_n(\tau) \otimes \widehat{\psi}^+_m(\tau') \rangle, n, m = k, D. \quad (11)$$

Their time evolution is considered on the Keldysh contour, C. The indexes $a, b = +, -$ denote the branches of the Keldysh contour, C_+ and C_-. Then the current is expressed as

$$I_L = 2e \sum_k \text{Tr}[\text{Re}\{T^+_L(t) \widehat{G}^{+-}_{Lk,1}(t,t)\}], \quad (12)$$

where $\widehat{G}^{+-}_{Lk,1}(t,t) = -i \langle \hat{T}_C \widehat{\psi}_{Lk}(t) \otimes [\widehat{P}_1 \widehat{\psi}_D(t)]^+ S_C \rangle_0$ is a mixed lesser Green's function. In the last definition the averaging is made over the states of the system without interaction (7). As a result the scattering matrix, $S_C = \hat{T}_C \exp\{-i \int_C d\tau \hat{H}_T(\tau)\}$, appears. Since the Hamiltonian of the device, $\hat{H}_D$, is formally the free-particle one, the rules for the second quantization operators can be utilized at the diagrammatic expansion of $\widehat{G}^{+-}_{Lk,1}(t,t)$. Hence the current is written as

$$I_L = 2e \int_C d\tau_1 \text{Tr}\big[\text{Re}\big\{\widehat{\Sigma}^{+a}_L(t - \tau_1) \widehat{P}_1 \widehat{G}^{a-}_D(\tau_1 - t) \widehat{P}^+_1\big\}\big], \quad (13)$$

where $\widehat{\Sigma}^{ab}_L(\tau - \tau') = T^+_L(\tau) \widehat{g}^{ab}_{Lk}(\tau - \tau') T_L(\tau')$ is the self-energy function characterizing the influence of the left lead on the structure; $\widehat{g}^{ab}_{Lk}(\tau - \tau')$ is the one-electron Green's function of the left lead. Taking into account the relations $\widehat{G}^{--}_{nm} = \widehat{G}^{+-}_{nm} - \widehat{G}^a_{nm}$, $\widehat{\Sigma}^{++}_L = \widehat{\Sigma}^r_L + \widehat{\Sigma}^{+-}_L$ (the indexes r and a mean "retarded" and "advanced" correspondingly) and using the Fourier transform, we obtain

$$I_L = 2e \int_{-\infty}^{+\infty} \frac{d\omega}{2\pi} \text{Tr}\big[\text{Re}\big\{\widehat{\Sigma}^r_L \widehat{P}_1 \widehat{G}^{+-}_D \widehat{P}^+_1 + \widehat{\Sigma}^{+-}_L \widehat{P}_1 \widehat{G}^a_D \widehat{P}^+_1\big\}\big]. \quad (14)$$

The Dyson and Keldysh equations for the full retarded and lesser Green's functions of the structure are

$$\begin{aligned} \widehat{G}^r_D &= \big((\omega + i\delta)\widehat{I} - \widehat{h}_D - \widehat{P}^+_1 \widehat{\Sigma}^r_L \widehat{P}_1 - \widehat{P}^+_4 \widehat{\Sigma}^r_R \widehat{P}_4\big)^{-1}, \\ \widehat{G}^{+-}_D &= \widehat{G}^r (\widehat{P}^+_1 \widehat{\Sigma}^{+-}_L \widehat{P}_1 + \widehat{P}^+_4 \widehat{\Sigma}^{+-}_R \widehat{P}_4) \widehat{G}^a, \\ \widehat{G}^a_D &= \big(\widehat{G}^r_D\big)^+. \end{aligned} \quad (15)$$

The retarded and lesser self-energy functions are given by

$$\begin{aligned} \widehat{\Sigma}^r_{L(R)} &= -\frac{i}{2} \text{diag}(\Gamma_{L(R)\uparrow}, \Gamma_{L(R)\downarrow}), \\ \widehat{\Sigma}^{+-}_{L(R)} &= if\left(\omega \pm \frac{eV}{2}\right) \text{diag}(\Gamma_{L(R)\uparrow}, \Gamma_{L(R)\downarrow}), \end{aligned} \quad (16)$$

where $\Gamma_{L(R)\sigma}(\omega) = \pi t^2_{L(R)} \rho_{L(R)\sigma}(\omega)$ is the coupling strength between the structure and the left (right) lead characterized by its density of states $\rho_{L(R)\sigma}(\omega) = \sum_k \delta(\omega - \xi_{k\sigma})$; $f(\omega \pm \frac{eV}{2})$ is the Fermi distribution function. In this study the leads are paramagnetic metals and treated in the wideband limit, i.e., $\Gamma_{L(R)\sigma} = \text{constant}$. After substituting (16) into (14) and using the relation $i(\widehat{G}^r_D - \widehat{G}^a_D) = \widehat{G}^r_D(\Gamma_L \widehat{P}^+_1 \widehat{P}_1 + \Gamma_R \widehat{P}^+_4 \widehat{P}_4) \widehat{G}^a_D$ [48] the final general expression describing

the current can be written as follows:

$$I_L = e\int_{-\infty}^{+\infty}\frac{d\omega}{2\pi}\mathrm{Tr}[\widehat{T}(\omega)][f(\omega - eV/2) - f(\omega + eV/2)], \tag{17}$$

where $\widehat{T}(\omega) = \Gamma_L\Gamma_R\widehat{G}^r_{14}(\widehat{G}^r_{14})^+$ is the matrix transmission coefficient; $\widehat{G}^r_{14} = \widehat{P}_1\widehat{G}^r_D\widehat{P}^+_4$. Note that an expression similar to (17) for current proportional to an effective transmission coefficient can be obtained for multilevel structures by exact diagonalization in the atomic representation [49,50].

In further numerical calculations the system will be considered at low temperatures. Moreover, in this study we will be interested in the behavior of the differential conductance, $G = dI_L/dV$, as a function of the gate voltage, ε_D (hereinafter we suppose that $\epsilon_{j\sigma} = \varepsilon_D$), at low bias (the so-called linear regime). Consequently, expanding $f(\omega \pm eV/2)$ into the Taylor series and taking into account $-df(\omega)/d\omega \approx \delta(\omega)$ we get the Landauer-Buttiker formula

$$G = G_0\mathrm{Tr}[\widehat{T}(\varepsilon_D,\omega = 0)], \tag{18}$$

where $G_0 = e^2/h$ is the conductance quantum. The total density of states (TDOS) is given by

$$\rho = \frac{i}{2\pi}\mathrm{Tr}\big[G^r_D - G^a_D\big]. \tag{19}$$

IV. THE RETARDED GREEN'S FUNCTION OF THE QQD STRUCTURE WITH THE COULOMB INTERACTIONS

In this section we describe the effects of Coulomb interactions on the transport properties of the QQD structure. In order to achieve this we employ the equation-of-motion technique for the retarded Green's functions, $G^r_{i\sigma j\sigma'}(\omega) = \langle\langle a_{i\sigma}|a^+_{j\sigma'}\rangle\rangle$, which are the Fourier transform of $G^r_{i\sigma j\sigma'}(t,t') = -i\Theta(t-t')\langle\{a_{i\sigma}(t),a^+_{j\sigma'}(t')\}\rangle$. The equation for $G^r_{i\sigma j\sigma'}(\omega)$ is

$$z\langle\langle a_{i\sigma}|a^+_{j\sigma'}\rangle\rangle = \langle\{a_{i\sigma},a^+_{j\sigma'}\}\rangle + \langle\langle[a_{i\sigma},\hat{H}]|a^+_{j\sigma'}\rangle\rangle, \tag{20}$$

where $z = \omega + i\delta$ and $\hat{H}$ has the form (1). Since the 2nd and 3rd QDs are identical in the considered system we denote them by the indexes α and $\overline{\alpha}$. The indexes of the 1st and 4th QDs are β and $\overline{\beta}$ for the same reason. As a result the equation for $\langle\langle a_{\alpha\sigma}|a^+_{\alpha\sigma}\rangle\rangle$, $\langle\langle a_{\beta\sigma}|a^+_{\alpha\sigma}\rangle\rangle$, and $\langle\langle c_{L(R)k\sigma}|a^+_{\alpha\sigma}\rangle\rangle$ are

$$\begin{aligned}
&(z-\xi_\alpha)\langle\langle a_{\alpha\sigma}|a^+_{\alpha\sigma}\rangle\rangle\\
&\quad= 1 + U\langle\langle n_{\alpha\overline{\sigma}}a_{\alpha\sigma}|a^+_{\alpha\sigma}\rangle\rangle + V(\langle\langle n_{\overline{\alpha}\sigma}a_{\alpha\sigma}|a^+_{\alpha\sigma}\rangle\rangle\\
&\qquad+\langle\langle n_{\overline{\alpha\sigma}}a_{\alpha\sigma}|a^+_{\alpha\sigma}\rangle\rangle) + t_0\langle\langle a_{\overline{\alpha}\sigma}|a^+_{\alpha\sigma}\rangle\rangle + t(\alpha)(\langle\langle a_{\beta\sigma}|a^+_{\alpha\sigma}\rangle\rangle\\
&\qquad+\langle\langle a_{\overline{\beta}\sigma}|a^+_{\alpha\sigma}\rangle\rangle),(z-\xi_\beta)\langle\langle a_{\beta\sigma}|a^+_{\alpha\sigma}\rangle\rangle\\
&\quad= U\langle\langle n_{\beta\overline{\sigma}}a_{\beta\sigma}|a^+_{\alpha\sigma}\rangle\rangle + t(\alpha)\langle\langle a_{\alpha\sigma}|a^+_{\alpha\sigma}\rangle\rangle\\
&\qquad+t(\overline{\alpha})\langle\langle a_{\overline{\alpha}\sigma}|a^+_{\alpha\sigma}\rangle\rangle + t(\beta)\sum_k\langle\langle c_{L(R)k\sigma}|a^+_{\alpha\sigma}\rangle\rangle,\\
&(z-\xi_{k\sigma})\langle\langle c_{L(R)k\sigma}|a^+_{\alpha\sigma}\rangle\rangle = t(\beta)\langle\langle a_{\beta\sigma}|a^+_{\alpha\sigma}\rangle\rangle,
\end{aligned} \tag{21}$$

where $t(\alpha = 2) \equiv t_1$, $t(\alpha = 3) \equiv t_2$, $t(\beta = 1) \equiv t_L$, $t(\beta = 4) \equiv t_R$. In the above equations, besides the first-order Green's functions, which we are interested in, the second-order Green's functions $\langle\langle n_{\alpha\overline{\sigma}}a_{\alpha\sigma}|a^+_{\alpha\sigma}\rangle\rangle$, $\langle\langle n_{\overline{\alpha}\sigma}a_{\alpha\sigma}|a^+_{\alpha\sigma}\rangle\rangle$, $\langle\langle n_{\overline{\alpha\sigma}}a_{\alpha\sigma}|a^+_{\alpha\sigma}\rangle\rangle$, $\langle\langle n_{\beta\overline{\sigma}}a_{\beta\sigma}|a^+_{\alpha\sigma}\rangle\rangle$ appear. The equations for them generate third-order Green's functions, and so on. To receive the closed set of equations the decoupling scheme of You and Zheng [42,43,51] is used. This approximation is valid for temperatures higher than the Kondo temperature [52]. In this truncation procedure the intra- and interdot Coulomb correlations are taken into account beyond the Hartree-Fock approximation while spin-flip processes are neglected.

Solving the final system (A1), presented in the Appendix, and using the notations of [51], we get in the non-magnetic case, $\langle n_{i\sigma}\rangle = \langle n_{i\overline{\sigma}}\rangle$, $\langle a^+_{i\sigma}a_{j\sigma}\rangle = \langle a^+_{i\overline{\sigma}}a_{j\overline{\sigma}}\rangle$, the following expressions for the matrix elements of $\hat{G}^r_D$,

$$\begin{aligned}
G^r_{\alpha\alpha} &= \frac{C_\alpha\big(D_{\overline{\alpha}}D_\beta - 2t^2(\overline{\alpha})C_{\overline{\alpha}}C_\beta + \frac{i}{2}\Gamma C_\beta D_{\overline{\alpha}}\big)}{X_1 - 2X_2 + iY},\\
G^r_{\alpha\overline{\alpha}} &= \frac{C_\alpha C_{\overline{\alpha}}\big(t_0D_\beta + 2t(\alpha)t(\overline{\alpha})C_\beta + \frac{i}{2}\Gamma t_0C_\beta\big)}{X_1 - 2X_2 + iY},\\
G^r_{\alpha\beta} &= \frac{C_\alpha C_\beta(t(\alpha)D_{\overline{\alpha}} + t_0t(\overline{\alpha})C_{\overline{\alpha}})}{X_1 - 2X_2 + iY},\\
G^r_{\beta\beta} &= \frac{C_\beta(X_1 - X_2 + iY)}{\big(D_\beta + \frac{i}{2}\Gamma C_\beta\big)(X_1 - 2X_2 + iY)},\\
G^r_{\overline{\beta}\beta} &= \frac{C_\beta X_2}{\big(D_\beta + \frac{i}{2}\Gamma C_\beta\big)(X_1 - 2X_2 + iY)},
\end{aligned} \tag{22}$$

where

$$\begin{aligned}
&D_\alpha = b_{\alpha1}b_{\alpha2}b_{\alpha\sigma3}b_{\alpha\sigma4}, D_\beta = b_{\beta1}b_{\beta2},\\
&C_\beta = b_{\beta2} + U\langle n_{\beta\sigma}\rangle, C_\alpha = C_{\alpha1} + C_{\alpha2},\\
&C_{\alpha1} = b_{\alpha\sigma4}(b_{\alpha2}b_{\alpha\sigma3} + Ub_{\alpha\sigma3}\langle n_{\alpha\sigma}\rangle + 2Vb_{\alpha2}\langle n_{\overline{\alpha}\sigma}\rangle),\\
&C_{\alpha2} = UV(b_{\alpha2} + b_{\alpha\sigma3})(2\langle n_{\alpha\sigma}\rangle\langle n_{\overline{\alpha}\sigma}\rangle - \langle a^+_{\alpha\sigma}a_{\overline{\alpha}\sigma}\rangle^2),\\
&X_1 = D_\beta\big(D_\alpha D_{\overline{\alpha}} - t_0^2C_\alpha C_{\overline{\alpha}}\big),\\
&X_2 = C_\beta[t^2(\alpha)C_\alpha D_{\overline{\alpha}} + t^2(\overline{\alpha})C_{\overline{\alpha}}D_\alpha + 2t_0t(\alpha)t(\overline{\alpha})C_\alpha C_{\overline{\alpha}}],\\
&Y = \tfrac{1}{2}\Gamma C_\beta\big(D_\alpha D_{\overline{\alpha}} - t_0^2C_\alpha C_{\overline{\alpha}}\big).
\end{aligned} \tag{23}$$

The occupation numbers and correlators are found self-consistently using the kinetic equations in equilibrium:

$$\begin{aligned}
\langle n_{i\sigma}\rangle &= -\frac{1}{\pi}\int d\omega f(\omega)\mathrm{Im}\big[G^r_{ii}(\omega)\big],\\
\langle a^+_{i\sigma}a_{j\sigma}\rangle &= -\frac{1}{\pi}\int d\omega f(\omega)\mathrm{Im}\big[G^r_{ji}(\omega)\big], i,j = \alpha,\beta.
\end{aligned} \tag{24}$$

For the sake of simplicity we will analyze a symmetrical transport situation and use $\Gamma_L = \Gamma_R = t$ in energy units. In this article we consider the strong-coupling regime, $t = t_1$.

V. TRANSPORT PROPERTIES OF THE QQD DEVICE WITHOUT THE COULOMB INTERACTIONS

A. Isotropic QQD

We start the analysis with the case when the couplings between the left (right) QD and both QDs in the middle part are the same, $t_1 = t_2 = 1$ [53], and the temperature is close to zero, $k_BT = 10^{-6}t$.

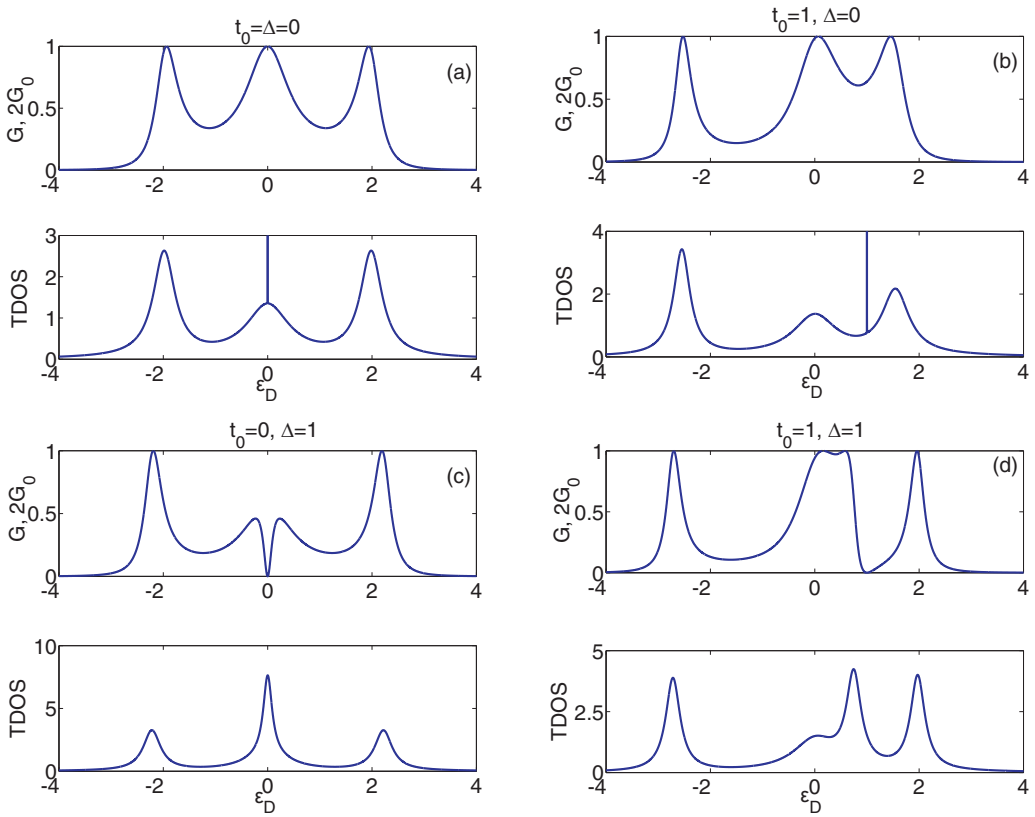

FIG. 2. The conductance and TDOS of the isotropic QQD: (a) $t_0 = \Delta = 0$; (b) $t_0 = 1, \Delta = 0$; (c) $t_0 = 0, \Delta = 1$; (d) $t_0 = 1, \Delta = 1$.

The simplest transport situation occurs if all levels have the same energy, $\xi_{1\sigma} = \xi_{2\sigma} = \xi_{3\sigma} = \xi_{4\sigma} = \varepsilon_D$, and $t_0 = 0$. The function $G(\varepsilon_D)$ is depicted in Fig. 2(a). The triple-peak structure (TPS) of the conductance can be easily understood since the system can be treated as the one consisting of two arms each composed of three coupled QDs. The corresponding TDOS has maxima at the same positions of ε_D. Additionally, the bound state in continuum (BIC) appears at $\varepsilon_D = 0$ [54,55]—the sharp peak with nearly zero width due to the $i\delta$ term in $\widehat{G}^r_D$ (15). The position of the BIC depends on t_0. In particular it shifts toward higher energies when t_0 increases [see TDOS in Fig. 2(b)]. Simultaneously the conductance spectrum does not contain corresponding features that are exactly the BIC's properties. In contrast to [53] we show that there is more than one way to make a finite lifetime of this state for such a system. The first of these is to realize two nonequivalent transport channels by means of the energy shift Δ, $\xi_{2(3)\sigma} = \varepsilon_D \pm \Delta$ [53]. As a result the destructive interference of the electronic waves propagating along these two paths gives rise to the Fano antiresonance [39] in the conductance spectrum and the resonance with finite width in the TDOS at $\varepsilon_D = 0$ [see Fig. 2(c)]. If $t_0 \neq 0$ the Fano antiresonance transforms to the Fano-Feshbach asymmetrical peak in the conductance spectrum in Fig. 2(d).

B. Anisotropic QQD

Let us consider the transport regime where the couplings between the QDs, t_1, t_2, t_0, are different and $t_1 \gg t_2, t_0$. Such an anisotropy is more convenient for real systems and the inequality between parameters can be even enhanced by the EPE. When $t_0 = \Delta = 0$ the conductance behaves similarly to the isotropic case [compare Figs. 2(a) and 3(a)]. This can be explained by the fact that changing the t_2 implies variation of the heights of the corresponding tunnel barriers only and does not affect the phase of the wave propagating along the bottom path. Thus, the interference of the waves passing in the two arms of the QQD structure leads to the conductance which differs from the isotropic one only quantitatively. If $t_0 \neq 0$ numerical calculations show that the anisotropy is the new mechanism leading to the Fano-Feshbach resonance along with the above-described one [53]. The simple explanation of this effect is based on the interpretation of the 2nd and 3rd QDs as an artificial molecule, a dimer [56,57]. The dimer has bonding and antibonding eigenstates which in general couple to other part of the system unequally. Then a more broadened level is treated as a continuum or nonresonant channel whereas a less broadened level plays the role of a discrete level or resonant channel in the original Fano picture [39]. The phase of the wave function in the nonresonant channel changes slightly as the energy passes an interval $\sim\Gamma$, where Γ is the broadening of the discrete level. However, the phase in the resonant channel shifts by $\sim\pi$ at the same energy interval. Consequently, the Fano-Feshbach resonant asymmetrical peak appears as a result of constructive and destructive interference at this energy range around the discrete level. Following [56] in the case of $\Delta = 0$, the coupling with one of the molecular states is absent without the anisotropy, $t_1 = t_2$, and there is no Fano-Feshbach effect [see Fig. 2(b)].

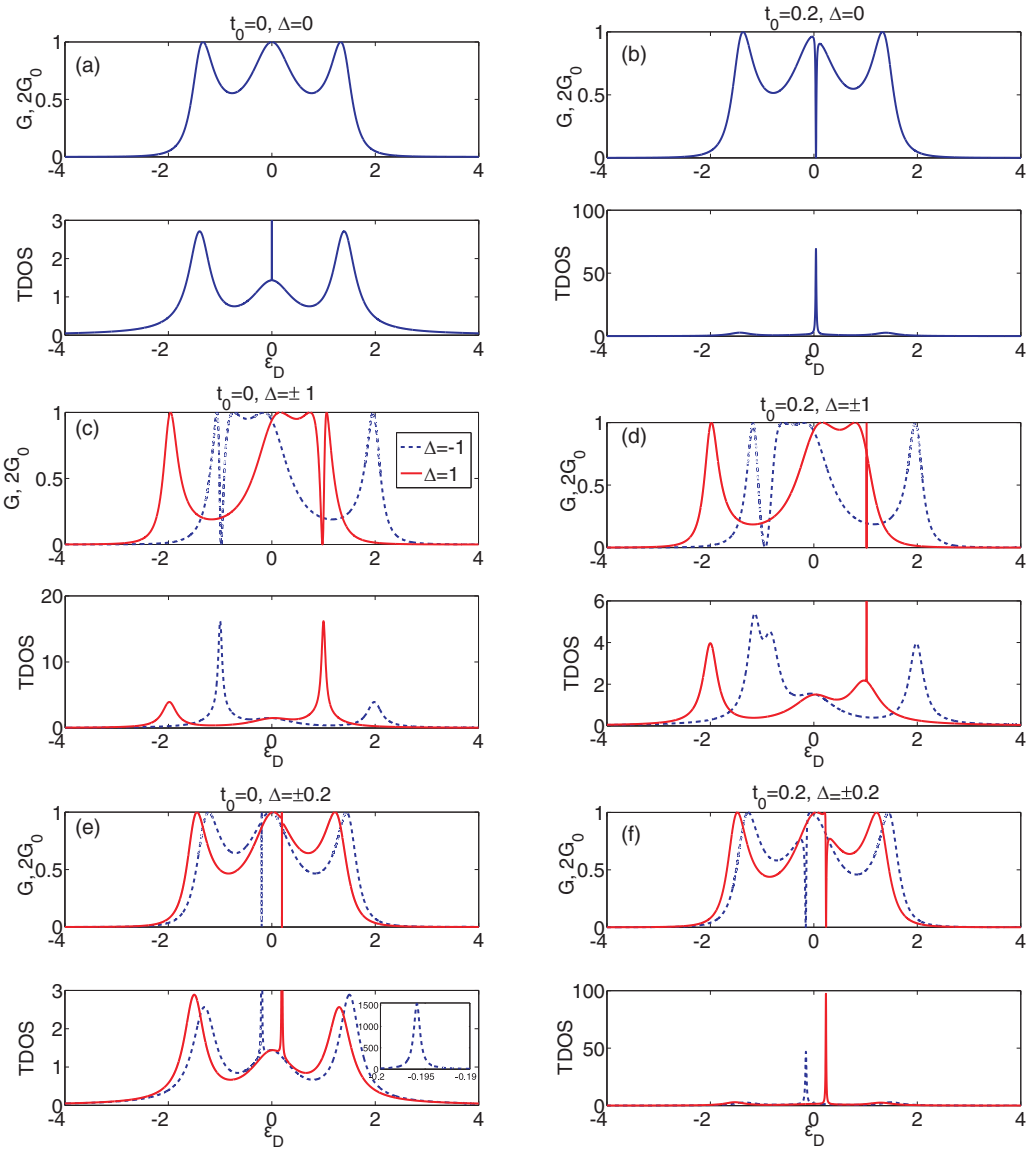

FIG. 3. The conductance and TDOS of the anisotropic QQD, $t_2 = 0.1$: (a) $t_0 = \Delta = 0$; (b) $t_0 = 0.2, \Delta = 0$; (c) $t_0 = 0, \Delta = \pm 1$; (d) $t_0 = 0.2, \Delta = \pm 1$; (e) $t_0 = 0, \Delta = \pm 0.2$; (f) $t_0 = 0.2, \Delta = \pm 0.2$.

In the opposite case the anisotropy induces the corresponding antiresonance as depicted in Fig. 3(b). If $\Delta \neq 0$ the coupling with both bonding and antibonding states does not equal zero even though $t_1 = t_2$ and the Fano-Feshbach resonance occurs [see Figs. 2(c), 2(d)] [57]. The anisotropy in this case leads to the change of the shape and width of the resonance and its dependence on the sign of Δ [see solid and dashed curves in Figs. 3(c)–3(f) for $\Delta = \pm 1$, respectively]. Specifically, the significant difference is observed in Fig. 3(d) where the wide resonance corresponds to $\xi_{2\sigma} < \xi_{3\sigma}$ and the very narrow one to $\xi_{2\sigma} > \xi_{3\sigma}$. The symmetry of the Fano-Feshbach resonance position is broken if $t_0 \neq 0$.

C. Temperature effects

If the temperature is comparable with the spacing between energy levels of the structure, i.e., $k_B T \sim \Delta, t_2, t_0$, the conductance can be calculated as

$$G = -G_0 \int_{-\infty}^{+\infty} d\omega \mathrm{Tr}[\widehat{T}(\omega)] \frac{\partial f}{\partial \omega}. \tag{25}$$

The temperature influence on the conductance is depicted in Fig. 4. If $k_B T \ll \Delta, t_2, t_0$, the smearing of the conductance, for example, the Fano-Feshbach asymmetrical peak, is not strong ($k_B T = 0.01$, dotted line). The dependence gradually becomes the Lorentzian-like curve with increasing $k_B T$.

VI. THE EFFECTS OF THE COULOMB INTERACTIONS

A. Isotropic QQD

The effect of the intradot, U, and interdot, V, Coulomb interactions on the conductance spectrum is displayed in detail in Figs. 5(a) and 5(b), respectively. The strong Coulomb repulsion of the electrons with different spin projections in each QD gives rise to the splitting of the TPS [dotted line in

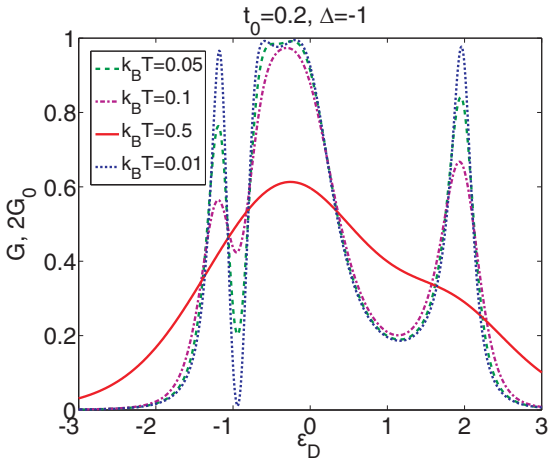

FIG. 4. The temperature effects on the conductance of the anisotropic QQD structure $t_2 = 0.1$, $t_0 = 0.2$, $\Delta = -1$.

Fig. 5(a)] and the appearance of the well-defined insulating band between two TPSs where G is close to zero [dash-dotted line in Fig. 5(a)]. It is clearly seen that the band forms without making the energy difference, Δ, which is influenced by external gate fields, and requires lesser quantity of QDs in comparison with [20,58]. Taking into account the interdot

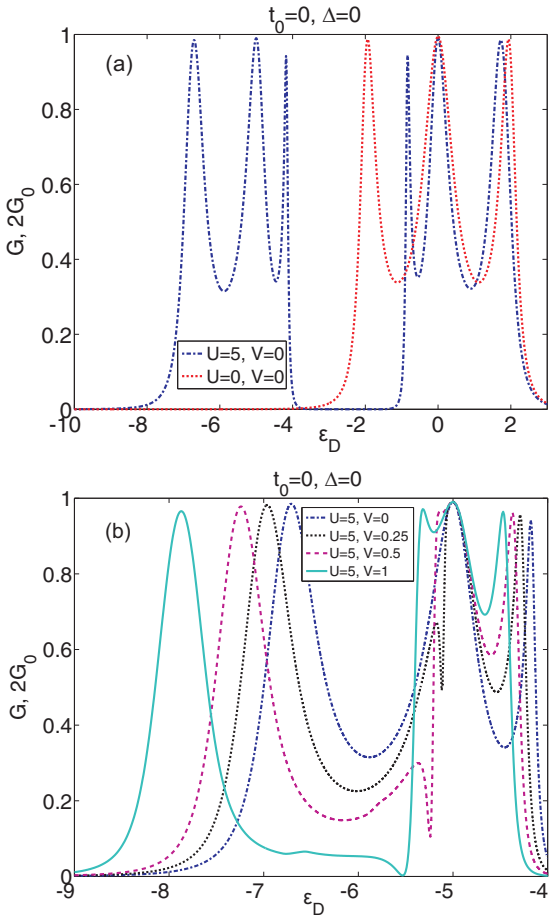

FIG. 5. The influence of the Coulomb interactions in the QQD on the conductance: (a) the effect of the intradot interactions, U; (b) the effect of the interdot interaction, V; $k_B T = 0.01$.

Coulomb interaction of the electrons in the middle part results in the splitting of the central peak in both TPSs as depicted in Fig. 5(b) by the example of the left TPS. It is worth noticing that the increase of V gives rise to the Fano antiresonance and the appearance of the sufficiently wide band with low conductance ($G \sim 0.1$ at $\varepsilon_D = -7$ to -5.5).

The TPS splitting effect is not symmetrical. The modification of the left and right TPSs is different for $V \neq 0$ [solid line in Fig. 6(a)]. The right TPS splitting leads to the broadening of the insulating band due to significant suppression of the first peak. If $U, V \neq 0$ and the carrier hopping between the 2nd and 3rd QDs is activated, the widths of the low-conductance band and insulating band become even larger as depicted in Fig. 6(b). As has already been discussed above, the nonzero energy shift Δ induces the Fano antiresonance or the asymmetrical peak in the central part of the TPS [dotted line in Fig. 6(c)]. This antiresonance is doubled for $U \neq 0, V = 0$ (dash-dotted line) and the low-conductance bands in both TPSs appear without the interdot Coulomb correlations (the regions $\varepsilon_D = -8$ to -6.5 and $\varepsilon_D = 0.5$ to 1.5). Finally, $V \neq 0$ results in two additional antiresonances (solid line) by analogy with the case $\Delta = 0$. As a prominent result in the right TPS the antiresonance, $G \simeq 0$, without the correlations (dotted line) is replaced by the resonance around $\varepsilon_D = 0$, $G \simeq 1$, with the correlations (solid line). If $t_0, \Delta = 1$ one more antiresonance appears at the left TPS and the one disappears at the right TPS [solid line in Fig. 6(d)].

The described behavior of the conductance is determined by the corresponding features of the occupation numbers. It can be easily illustrated in the simplest regime, $t_0 = \Delta = 0$. In the absence of all the Coulomb interactions the gate voltage dependencies of the side, $n_{1,4\sigma}$, and the central, $n_{2,3\sigma}$, QD occupations have three steps at the same positions as the resonances in the TPS [see dashed and solid lines in Fig. 7(a)]. If the intradot correlations are taken into account this staircase obtains three more steps at a distance U [Fig. 7(b)]. The interdot Coulomb interaction leads to the splitting of each central step of $n_{2,3\sigma}$ around $\varepsilon_D = -5,0$ [Fig. 7(c)] [42]. Importantly, the extensive areas where the occupations do not change correspond to the insulating and low-conductance bands in Figs. 5 and 6(a). In particular, the insulating band appears at the half-filling region. Lastly, the weak influence of the Coulomb correlations on the conductance at the high gate fields ($\varepsilon_D \geqslant 1$) is explained by the low occupation of the QQD's levels.

Since this work deals with the quantum transport in the strong-coupling regime it is important to discuss briefly possible manifestation of the Kondo effect. The rough estimation of the Kondo temperature, T_K, using the one for single quantum dot [52] gives comparable values with $k_B T$ and even higher values of T_K. At the same time, we suppose $\Gamma = t_1$ and the consistent consideration of spin correlations in the system should include antiferromagnetic interactions, $J \sim t_1^2/U$ or $J \sim t_1^2/\Delta$, between the electrons in the QQD structure. This problem has been well known for a long time, since Doniach's work [59]. In mesoscopics as was already shown for a double quantum dot such a competition can completely suppress the Kondo resonance at half filling [60]. The question of the interplay between these two regimes is beyond the scope of this work and seems to be very intriguing for future analysis.

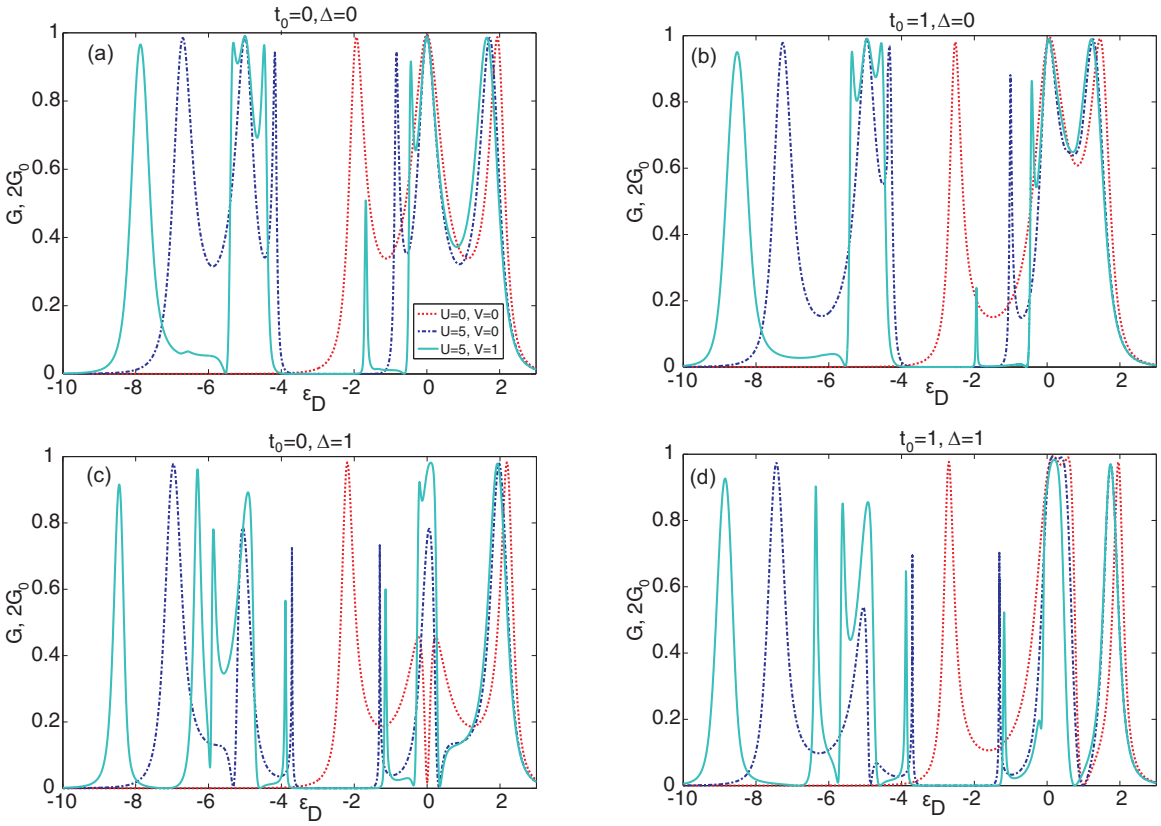

FIG. 6. The conductance of the isotropic QQD, $k_BT = 0.01$: (a) $t_0 = \Delta = 0$; (b) $t_0 = 1, \Delta = 0$; (c) $t_0 = 0, \Delta = 1$; (d) $t_0 = 1, \Delta = 1$.

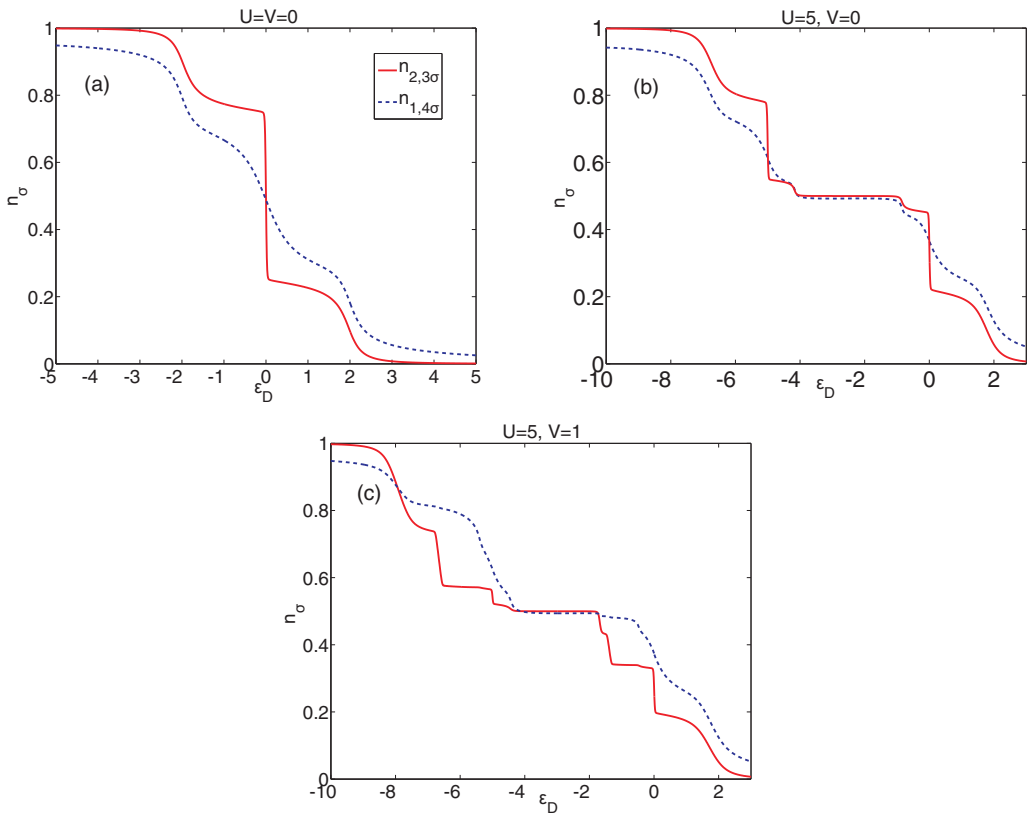

FIG. 7. The gate-field dependence of occupation numbers of the isotropic QQD, $t_0 = \Delta = 0$, $k_BT = 0.01$: (a) $U = V = 0$; (b) $U = 5$, $V = 0$; (c) $U = 5, V = 1$.

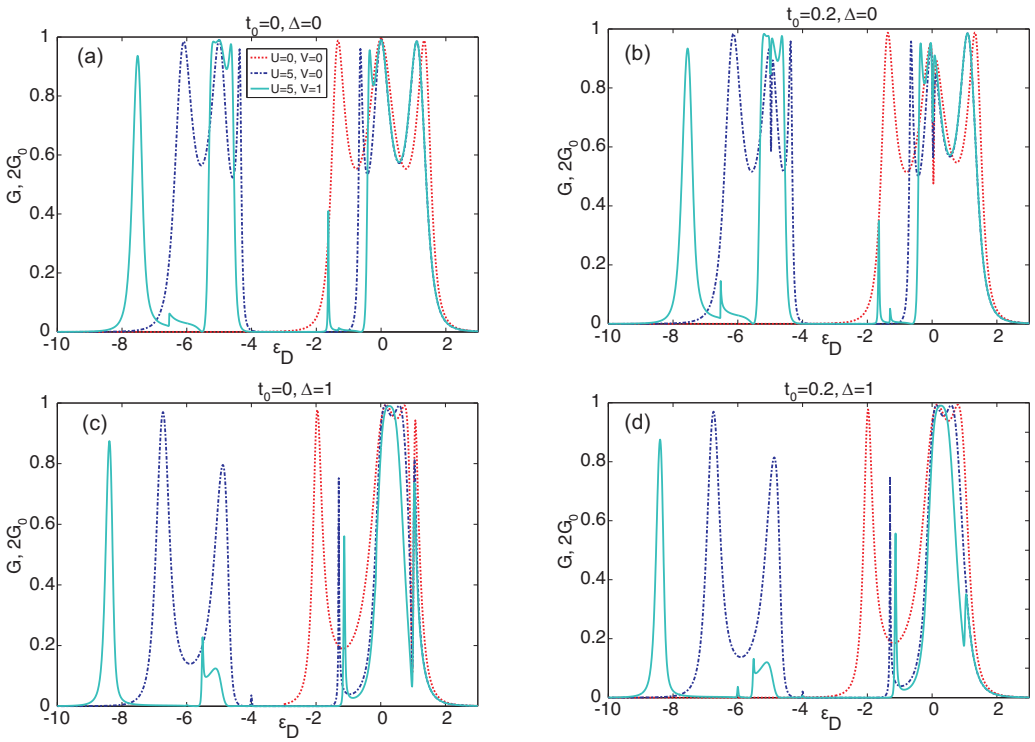

FIG. 8. The conductance of the anisotropic QQD, $t_2 = 0.1$, $k_BT = 0.01$: (a) $t_0 = \Delta = 0$; (b) $t_0 = 0.2, \Delta = 0$; (c) $t_0 = 0, \Delta = 1$; (d) $t_0 = 0.2, \Delta = 1$.

B. Anisotropic QQD

When the anisotropy of the hopping integrals takes place the effect of the interdot tunneling in the central part on the conductance is not strong in comparison with the isotropic situation: the low-conductance band at the left TPS in Fig. 8(b) becomes narrower. The influence of the Coulomb correlations results in the same features. However, the combination of the Coulomb interactions with the energy shift Δ can dramatically change the conductance [compare dash-dotted and solid lines in Figs. 8(c), 8(d)]. We can clearly see that the big insulating band occurs with a small conductance peak emerging in the middle as a result of the significant suppression of the left TPS. It can be qualitatively attributed to the higher occupation of the 3QD ($\Delta > 0$) and weaker kinetic processes in the bottom arm (1QD-3QD-4QD) leading to the enhancement of the Fano destructive interference due to V. At the same time, before the half filling the right TPS is less modified in consequence of the low total occupation of the QQD structure at high fields. Thus the EPE, which is expected in the system with the heavy and light carriers due to the strong interdot Coulomb interaction V and/or the hybridization between them t_0, and gate fields can considerably modify the conductance by the significant suppression of the TPS. Note that for all the values of Δ satisfying the inequality $2t_1 > \Delta$ the overlap between the effective heavy and light bands remains and we are in the situation suitable for the EPE [25].

VII. CONCLUSION

We have considered the spectral and transport properties of the QQD structure at low temperatures, low bias, and the strong-coupling regime. The treatment of the problem was based on the nonequilibrium Green's functions and the tight-binding approximation. It is found that there is more than one way to observe the Fano effect in the system. The first of these has already been mentioned and consists of making two nonequivalent paths for electron waves by the energy shift Δ [53]. Additionally we showed that the anisotropy of the kinetic processes in the system, $t_1 \neq t_2$, leads to the Fano-Feshbach asymmetrical peak for $t_0 \neq 0$ even though $\Delta = 0$. The effect is explained in terms of resonant interaction between the bonding and antibonding states in the system. This scenario of the Fano effect seems to be more attractive for experimental observation since it does not need a gate field. The anisotropy results in the dependence of the shape and width of the Fano-Feshbach resonance on the sign of Δ as well. In our system the anisotropy models the joint effect of both adjustable tunnel barriers and the EPE-like physics. The last can be induced by the strong interdot Coulomb interaction V of the heavy and light carriers and/or their hybridization t_0.

The problem of the influence of the Coulomb correlations on quantum transport in the QQD device was solved using the equation-of-motion technique for the retarded Green's functions. We applied the decoupling scheme of You and Zheng [42,43] which allows us to take into account the intra- and interdot Coulomb correlations beyond the Hartree-Fock approximation in nonmagnetic case. We demonstrated that the QQD structure has a wide region of zero conductance with steep edges separating two TPSs if the intradot Coulomb interactions in each dot are allowed. This effect has been considered earlier for more sophisticated QD-based devices [20,58]. The interdot Coulomb correlations between the central QDs results

in the broadening of this band and the occurrence of the band with low conductance in the left TPS due to the Fano antiresonances. When the hopping between the central QDs is also permitted the bands become even wider. Furthermore, the conductance of the anisotropic QQD device can be remarkably modified by changing Δ if the interdot Coulomb repulsion is taken into account.

ACKNOWLEDGMENTS

We acknowledge fruitful discussions with P. I. Arseyev, N. S. Maslova, V. N. Mantsevich, and R. Sh. Ikhsanov. This work was financially supported by the Comprehensive programme SB RAS No. 0358-2015-0007, the RFBR, Government of Krasnoyarsk Territory, Krasnoyarsk Region Science and Technology Support Fund, Projects No. 15-02-03082, No. 15-42-04372, No. 16-42-243056, and No. 16-42-242036. M.Yu.K. thanks the Program of Basic Research of the National Research University Higher School of Economics for support.

APPENDIX

In this appendix, the final system of equations for the retarded Green's functions of the QQD structure with the Coulomb correlations is presented,

$$\langle\langle a_{\alpha\sigma}|a^{+}_{\alpha\sigma}\rangle\rangle = (g_{\alpha\sigma} - K_{\alpha\sigma})(1 + t_0\langle\langle a_{\bar{\alpha}\sigma}|a^{+}_{\alpha\sigma}\rangle\rangle + t(\alpha)[\langle\langle a_{\beta\sigma}|a^{+}_{\alpha\sigma}\rangle\rangle + \langle\langle a_{\bar{\beta}\sigma}|a^{+}_{\alpha\sigma}\rangle\rangle]),$$

$$\langle\langle a_{\beta\sigma}|a^{+}_{\alpha\sigma}\rangle\rangle = \frac{g^{(0)}_{\beta\sigma}}{1 - \Sigma_\beta g^{(0)}_{\beta\sigma}}[t(\alpha)\langle\langle a_{\alpha\sigma}|a^{+}_{\alpha\sigma}\rangle\rangle + t(\bar{\alpha})\langle\langle a_{\bar{\alpha}\sigma}|a^{+}_{\alpha\sigma}\rangle\rangle], \tag{A1}$$

where

$$\begin{aligned}
K_{\alpha\sigma} &= \frac{UV\langle a^{+}_{\alpha\bar{\sigma}}a_{\bar{\alpha}\bar{\sigma}}\rangle^2}{b_{\alpha1}b_{\alpha\sigma4}}\left(\frac{1}{b_{\alpha2}} + \frac{1}{b_{\alpha\sigma3}}\right),\\
g_{\alpha\sigma} &= g^{(0)}_{\alpha\sigma} + \frac{V}{b_{\alpha1}}\left[g^{(1)}_{\alpha\sigma} + g^{(2)}_{\alpha\sigma} + \frac{U}{b_{\alpha2}}g^{(3)}_{\alpha\sigma}\right],\\
g^{(0)}_{\alpha\sigma} &= \frac{1 - \langle n_{\alpha\bar{\sigma}}\rangle}{b_{\alpha1}} + \frac{\langle n_{\alpha\bar{\sigma}}\rangle}{b_{\alpha2}},\\
g^{(1)}_{\alpha\sigma} &= \frac{(1 - \langle n_{\alpha\bar{\sigma}}\rangle)\langle n_{\bar{\alpha}\sigma}\rangle}{b_{\alpha\bar{\sigma}3}} + \frac{\langle n_{\alpha\bar{\sigma}}\rangle\langle n_{\bar{\alpha}\sigma}\rangle}{b_{\alpha\bar{\sigma}4}},\\
g^{(2)}_{\alpha\sigma} &= \frac{(1 - \langle n_{\alpha\bar{\sigma}}\rangle)\langle n_{\bar{\alpha}\bar{\sigma}}\rangle}{b_{\alpha\sigma3}} + \frac{\langle n_{\alpha\bar{\sigma}}\rangle\langle n_{\bar{\alpha}\bar{\sigma}}\rangle}{b_{\alpha\sigma4}},\\
g^{(3)}_{\alpha\sigma} &= \frac{\langle n_{\alpha\bar{\sigma}}\rangle\langle n_{\bar{\alpha}\sigma}\rangle}{b_{\alpha\bar{\sigma}4}} + \frac{\langle n_{\alpha\bar{\sigma}}\rangle\langle n_{\bar{\alpha}\bar{\sigma}}\rangle}{b_{\alpha\sigma4}},\\
g^{(0)}_{\beta\sigma} &= g^{(0)}_{\alpha\to\beta,\sigma}, \Sigma_\beta = -i\frac{t}{2},\\
b_{\alpha1} &= z - \xi_\alpha, b_{\alpha2} = b_{\alpha1} - U,\\
b_{\alpha\sigma3} &= b_{\alpha1} - V(1 + \langle n_{\bar{\alpha}\sigma}\rangle), b_{\alpha\sigma4} = b_{\alpha\sigma3} - U.
\end{aligned} \tag{A2}$$

[1] K. Kikoin and Y. Avishai, Phys. Rev. Lett. **86**, 2090 (2001).
[2] A. Oguri and A. C. Hewson, J. Phys. Soc. Jpn. **74**, 988 (2005).
[3] F. Delgado, Y.-P. Shim, M. Korkusinski, L. Gaudreau, S. A. Studenikin, A. S. Sachrajda, and P. Hawrylak, Phys. Rev. Lett. **101**, 226810 (2008).
[4] R. Hanson, L. P. Kouwenhoven, J. R. Petta, S. Tarucha, and L. M. K. Vandersypen, Rev. Mod. Phys. **79**, 1217 (2007).
[5] I. P. Gimenez, C.-Y. Hsieh, M. Korkusinski, and P. Hawrylak, Phys. Rev. B **79**, 205311 (2009).
[6] M. E. Torio, K. Hallberg, S. Flach, A. E. Miroshnichenko, and M. Titov, Eur. Phys. J. B **37**, 399 (2004).
[7] M. B. Haider, J. L. Pitters, G. A. DiLabio, L. Livadaru, J. Y. Mutus, and R. A. Wolkow, Phys. Rev. Lett. **102**, 046805 (2009).
[8] C.-Y. Hsieh, Y.-P. Shim, M. Korkusinski, and P. Hawrylak, Rep. Prog. Phys. **75**, 114501 (2012).
[9] T. A. Baart, N. Jovanovic, C. Reichl, W. Wegscheider, and L. M. K. Vandersypen, Appl. Phys. Lett. **109**, 043101 (2016).
[10] R. Thalineau, S. Hermelin, A. D. Wieck, C. Bauerle, L. Saminadayar, and T. Meunier, Appl. Phys. Lett. **101**, 103102 (2012).
[11] J. von Stecher, E. Demler, M. D. Lukin, and A. M. Rey, New J. Phys. **12**, 055009 (2010).
[12] P. Barthelemy and L. M. K. Vandersypen, Ann. Phys. **525**, 808 (2013).
[13] A. Mizel and D. A. Lidar, Phys. Rev. B **70**, 115310 (2004).
[14] V. W. Scarola and S. Das Sarma, Phys. Rev. A **71**, 032340 (2005).
[15] D. Venturelli, R. Fazio, and V. Giovannetti, Phys. Rev. Lett. **110**, 256801 (2013).
[16] Y. Nisikawa and A. Oguri, Phys. Rev. B **73**, 125108 (2006).
[17] I. Ozfidan, A. H. Trojnara, M. Korkusinski, and P. Hawrylak, Solid State Commun. **172**, 15 (2013).
[18] Z.-T. Jiang and Q.-Z. Han, Phys. Rev. B **78**, 035307 (2008).
[19] A. M. Lobos and A. A. Aligia, Phys. Rev. Lett. **100**, 016803 (2008).
[20] H.-H. Fu and K.-L. Yao, Appl. Phys. Lett. **100**, 013502 (2012).
[21] D. M. News and M. Read, Adv. Phys. **36**, 799 (1987).
[22] P. Fulde, *Electron Correlations in Molecules and Solids* (Springer, Berlin, 1983).
[23] P. Coleman, Phys. Rev. B **35**, 5072 (1987).
[24] H. Keitler and N. Grewe, in *Valence Fluctuations in Solids*, edited by L. M. Falicov, W. Hanke, and M. B. Maple (North-Holland, New York, 1981), p. 451.
[25] M. Yu. Kagan and V. V. Val'kov, J. Theor. Exp. Phys. **113**, 156 (2011).
[26] M. Yu. Kagan and V. V. Val'kov, Low Temp. Phys. **37**, 69 (2011); and also in *A Lifetime in Magnetism and Superconductivity: A Tribute to Professor David Shoenberg*, edited by G. Lonzarich, S. S. Saxena, V. A. Sirenko, and V. V. Eremenko (Cambridge Scientific Publishers, Cambridge, 2017).
[27] P. W. Anderson, J. Phys. C **3**, 2436 (1970).
[28] J. Kondo, Prog. Theor. Phys. **32**, 37 (1964).
[29] G. Iche and P. Nozieres, Physica A **91**, 485 (1978).
[30] Yu. Kagan and N. V. Prokof'ev, JETP **63**, 1276 (1986).
[31] Yu. Kagan and N. V. Prokof'ev, JETP **66**, 211 (1987).

[32] D. A. Mahan, Phys. Rev. **163**, 612 (1967).
[33] P. Nozieres and L. T. de Dominicis, Phys. Rev. **178**, 1097 (1969).
[34] P. W. Anderson, Phys. Rev. Lett. **18**, 1049 (1958).
[35] S. V. Demishev, A. N. Samarin, J. Huang, V. V. Glushkov, I. I. Lobanova, N. E. Sluchanko, N. M. Chubova, V. A. Dyadkin, S. V. Grigoriev, M. Yu. Kagan, J. Vanacken, and V. V. Moshchalkov, JETP Lett. **104**, 116 (2016).
[36] K. A. Matveev and A. I. Larkin, Phys. Rev. B **46**, 15337 (1992).
[37] P. I. Arseev and N. S. Maslova, JETP **75**, 575 (1992).
[38] P. I. Arseev, N. S. Maslova, and V. N. Mantsevich, JETP Lett. **94**, 390 (2011); JETP **115**, 141 (2012).
[39] U. Fano, Phys. Rev. **124**, 1866 (1961).
[40] H. Feshbach, Ann. Phys. **19**, 287 (1962).
[41] Z. G. Yu, D. L. Smith, A. Saxena, R. L. Martin, and A. R. Bishop, Phys. Rev. B **63**, 085202 (2001).
[42] J. Q. You and H.-Z. Zheng, Phys. Rev. B **60**, 8727 (1999).
[43] J. Q. You and H.-Z. Zheng, Phys. Rev. B **60**, 13314 (1999).
[44] M. Friesen, P. Rugheimer, D. E. Savage, M. G. Lagally, D. W. van der Weide, R. Joynt, and M. A. Eriksson, Phys. Rev. B **67**, 121301(R) (2003).
[45] D. Rogovin and D. J. Scalapino, Ann. Phys. (N.Y.) **86**, 1 (1974).
[46] L. V. Keldysh, JETP **20**, 1018 (1965).
[47] S. Datta, *Electronic Transport in Mesoscopic Systems* (Cambridge University Press, New York, 1995).
[48] S. Datta, *Quantum Transport: Atom to Transistor* (Cambridge University Press, New York, 2005).
[49] V. V. Val'kov, S. V. Aksenov, and E. A. Ulanov, JETP Lett. **98**, 403 (2013).
[50] V. V. Val'kov, S. V. Aksenov, and E. A. Ulanov, JETP **119**, 124 (2014).
[51] G. Rajput, S. Chand, P. K. Ahluwalia, and K. C. Sharma, Physica B **405**, 4323 (2010).
[52] C. Lacroix, J. Phys. F **11**, 2389 (1981).
[53] J.-X. Yan and H.-H. Fu, Physica B **410**, 197 (2006).
[54] A. Volya and V. Zelevinsky, Phys. Rev. C **67**, 054322 (2003).
[55] A. F. Sadreev, E. N. Bulgakov, and I. Rotter, Phys. Rev. B **73**, 235342 (2006).
[56] H. Lu, R. Lu, and B.-F. Zhu, Phys. Rev. B **71**, 235320 (2005).
[57] Y.-S. Liu, H. Chen, and X.-F. Yang, J. Phys.: Condens. Matter. **19**, 246201 (2007).
[58] W. Gong, Y. Zheng, Y. Liu, and T. Lu, J. Phys. F **73**, 245329 (2006).
[59] S. Doniach, Physica B **91**, 231 (1977).
[60] L. C. Ribeiro, E. Vernek, G. B. Martins, and E. V. Anda, Phys. Rev. B **85**, 165401 (2012).